Hindawi Publishing Corporation
Modelling and Simulation in Engineering
Volume 2013, Article ID 932094, 12 pages
http://dx.doi.org/10.1155/2013/932094

Research Article

Prediction of Surface Roughness When End Milling *Ti6Al4V* Alloy Using Adaptive Neurofuzzy Inference System

Salah Al-Zubaidi, Jaharah A. Ghani, and Che Hassan Che Haron

Department of Mechanical and Material Engineering, Faculty of Engineering and Built Environment, Universiti Kebangsaan Malaysia, 43600 Bangi, Selangor, Malaysia

Correspondence should be addressed to Salah Al-Zubaidi; salah@eng.ukm.my

Received 30 May 2013; Revised 17 August 2013; Accepted 17 August 2013

Academic Editor: ShengKai Yu

Surface roughness is considered as the quality index of the machine parts. Many diverse techniques have been applied in modelling metal cutting processes. Previous studies have revealed that artificial intelligence techniques are novel soft computing methods which fit the solution of nonlinear and complex problems like metal cutting processes. The present study used adaptive neurofuzzy inference system for the purpose of predicting the surface roughness when end milling *Ti6Al4V* alloy with coated (PVD) and uncoated cutting tools under dry cutting conditions. Real experimental results have been used for training and testing of *ANFIS* models, and the best model was selected based on minimum root mean square error. A generalized bell-shaped function has been adopted as a membership function for the modelling process, and its numbers were changed from 2 to 5. The findings provided evidence of the capability of *ANFIS* in modelling surface roughness in end milling process and obtainment of good matching between experimental and predicted results.

1. Introduction

Ti6Al4V alloy is an important super alloy being subjected to diverse applications in the biomedical, aerospace, and chemical industries because of its properties and features such as high specific strength, high corrosion resistance, and good performance at high temperatures. However, since it has certain features such as its chemical reactivity, low thermal conductivity (this reduces heat dissipation from the cutting zone), high strength and hardness, and its low modulus of elasticity which make it more flexible than metals such as steel, *Ti6Al4V* alloy is regarded to be difficult to machine [1, 2]. Therefore, choosing the cutting parameters for end milling alloys such as this is considered as a critical process. High quality products at a reasonable cost have been increasingly demanded or required, which has compelled manufacturers into fierce competition. Thus, to evaluate the quality of products, it is important to consider surface finish as an important factor in such evaluation. The purpose of using surface roughness (R_a) as an index is mostly to determine the surface finish in the machining process. In classifying modeling techniques for the prediction of R_a, there are three major categories, namely, experimental models, analytical models, and artificial intelligence- (AI-) based models [3]. Development of the first two categories or groups is possible to be carried out by using conventional approaches such as the statistical regression technique. However, for developing the last category, AI-based models, nonconventional approaches such as the artificial neural network (ANN), fuzzy logic (FL), and genetic algorithm (GA) are usually used for this purpose [4]. In manufacturing, the importance of the milling process comes after turning in the ranks, and there is a possibility of creating and producing complex geometry by using the end milling process [5]. Milling is stated to be different from turning in that it is considered as a multiple cutting point process which is categorized into slab, face milling, and end milling. It comes in one of two modes either up or down. Moreover, the surface finish generated in milling significantly impacts or affects a material's fatigue resistance and functional performance. Surface roughness is also regarded as a product quality index, and it is sometimes demanded in product specifications [6].

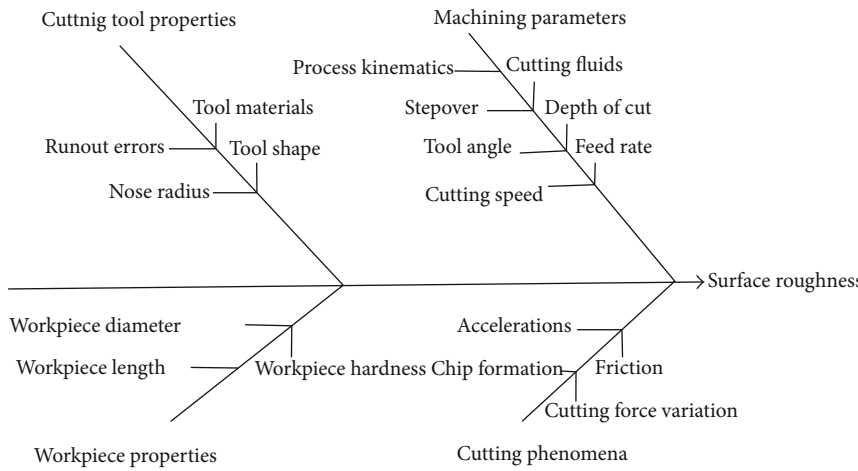

Figure 1: Factors affecting surface roughness [6].

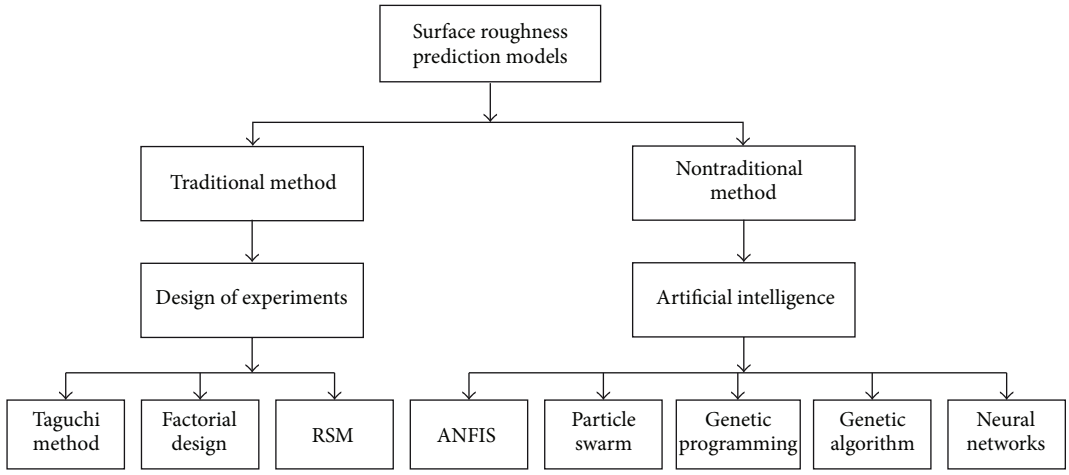

Figure 2: Surface roughness prediction research areas [7].

As displayed in Figure 1, interconnected parameters such as tool wear, cutting speed, feed rate, and radial and axial depth of cut, are found to significantly affect the surface roughness of a machined part [8]. Figure 2 shows the major areas for surface roughness prediction which have been used as the basics upon which research has been founded, and they include design of experiments, processes, materials, and artificial techniques. Thus, it is expected that developing a realistic model for predicting this performance measure will assist researchers to reduce machining time and costs. Recent research has provided evidence of the ability of AI-based models in modelling cutting processes.

One of those AI-based models as prove by such recent research is adaptive neuro-fuzzy inference system (ANFIS), which, as feature, combines the merits of fuzzy knowledge and function approximation of neural networks [10, 11]. It is stated that neural network is able to deal with imprecise data and can obtain low-level computational features, whereas fuzzy logic can provide researchers with high-level cognitive features and deal with some issues like natural language processing and approximate reasoning [11]. Based on previous research, the nonlinear relationship existing between input and output parameters in neural networks has not been revealed so far and cannot be accessed by the user, and, therefore, the importance of ANFIS is recognized as it can be used to overcome such weakness [12]. In study by Dweiri et al. [13] which aimed to model the down milling for predicting surface roughness of Alumic-79, the researchers employed ANFIS. They used two and four flutes, and findings revealed that the optimum value of surface roughness could be obtained using four flutes. In predicting workpiece surface roughness when end milling AA 6061 heat treatable aluminum alloy, Lo [14] used the same system, ANFIS, and the study involved 48 experiments for training and 24 for testing. It was found that obtaining high prediction accuracy was achieved when triangle membership function was used.

Göloğlu and Arslan [15] carried out a study for prediction of the surface roughness of milled 40CrMnNiMo8-6-4 alloy steel using zigzag motion for the four-flute cutter. First,

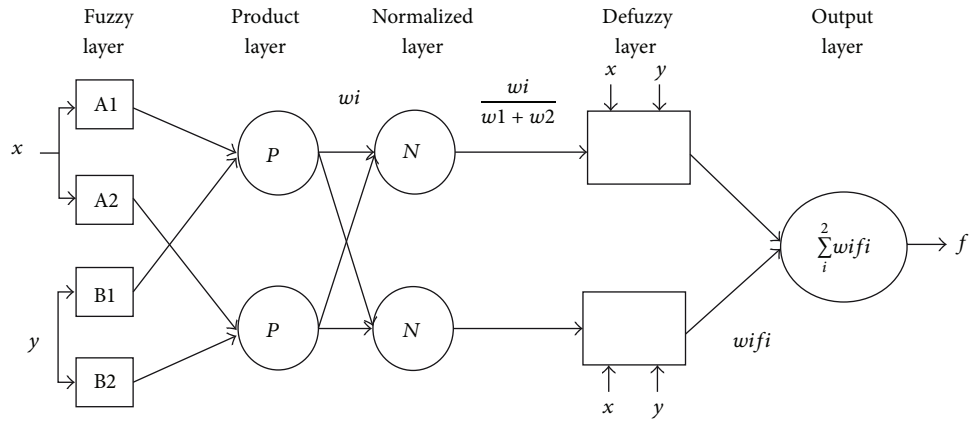

Figure 3: Adaptive neuro-fuzzy inference system [9].

the researchers developed three artificial models, namely, genetic programming (GP), artificial neural networks (ANN), and adaptive neurofuzzy inference system (ANFIS) models and then compared them. The experiments were designed by using Taguchi's orthogonal arrays. The best results were gained by using GP model with good accuracy. For modelling the surface roughness in end milling, Ho et al. [16] made integration of the ANFIS with hybrid Taguchi-genetic algorithm, learning algorithm by using Lo's experimental results [14]. The purpose was to test reliability of the proposed hybrid approach. In comparing their method with other previously reported ones in the literature, the researchers revealed their proposed method was slightly accurate than the others. In a study conducted by Uros et al. [17], the ANFIS model was proposed for the purpose of predicting flank wear using cutting force signal generated in end milling of Ck 45 and Ck 45 (XM) alloys using trapezoidal and triangular membership functions. Findings showed that there was a good consistency found between the experimental results and the ANFIS model. Dong and Wang [18] applied the ANFIS model with leave-one-out cross-validation method for prediction of surface roughness using also Lo's experimental results [14]. Based on a comparison between other literatures results and the results obtained by them through the ANFIS clustering method, the researchers gained better accuracy by using the proposed method than the others did. However, the deficiency of previous research is that no study has aimed to model the surface roughness of milled *Ti6Al4V* super alloy under dry cutting conditions by using the ANFIS, and this is a part of the contributions expected to be offered by the current study to this particular research area.

2. ANFIS Architecture

This section provides an illustration of the basic architecture of the ANFIS and its learning algorithm for the Sugeno fuzzy model. Assuming that the fuzzy inference system consists of two inputs m and n and one output y, for an initial order Sugeno fuzzy model, the followings expressing a typical rule set with two fuzzy if-then rules are taken into account [9, 14]:

Rule 1: If (m is $A1$) and (n is $B1$), then: $y1 = \alpha 1m + \beta 1n + \gamma 1$

Rule 2: If (m is $A2$) and (n is $B2$), then: $y2 = \alpha 2m + \beta 2n + \gamma 2$,

where $\alpha 1$, $\beta 1$, $\gamma 1$, $\alpha 2$, $\beta 2$, and $\gamma 2$ represent the linear parameters, and $A1$, $A2$, $B1$, and $B2$ symbolize the nonlinear parameters. As displayed in Figure 3, the corresponding equivalent ANFIS architecture is composed of five layers, namely, a fuzzy layer, a product layer, a normalized layer, a defuzzy layer, and a total output layer. Thus, the following subsections provide more detailed description of the functionality of each of these layers.

2.1. Layer 1: Fuzzy Layer

(i) Let $O1, i$ be the output of the ith node of layer 1.

(ii) Every node i in this layer is recognized as an adaptive node with a node function as follows:

$$\begin{aligned} O1, i &= \mu Ai\,(x) \quad \text{for } i = 1, 2 \quad \text{or} \\ O1, i &= \mu Bi\,(y) \quad \text{for } i = 1, 2, \end{aligned} \tag{1}$$

where x represents the input to node i and Ai refers to the linguistic label (small, large, etc.) which is related to this node function. In other words, $O1, i$ reflects the membership function of Ai and gives specification of the degree to which the given x satisfies the quantifier Ai. The most commonly used membership functions are bell-shaped and the Gaussian membership functions.

(iii) The bell-shaped membership function is given by

$$f\,(x, a, b, c) = \frac{1}{1 + \left(\left(x - c^{2b}\right)/a\right)}, \tag{2}$$

where the parameter b is usually positive. The parameter c provides a location of the centre of the curve.

(iv) The Gaussian membership function is expressed as follows:

$$A\,(x) = e^{(x-c)2/2\sigma^2}, \quad \text{where } 2\sigma 2 > 0. \tag{3}$$

(v) The parameters in layer 1 are referred to as the premise parameters.

2.2. Layer 2: Product Layer

(i) Each node in this layer has a prod t-norm operator which is used as a node function.

(ii) This layer makes a synthesis of the information transmitted by layer 1, makes multiplication of all the incoming signals, and sends the product out.

(iii) The output of the product layer is given by

$$O2,i = \mu Ai\,(x)\,\mu Bi\,(y)\,. \tag{4}$$

(iv) Each node in this layer functions as a measure of strength of the rule.

(v) The output of this layer acts as the weight functions.

2.3. Layer 3: Normalized Layer

(i) Each node in this layer makes normalization of the weight functions gained from the previous product layer.

(ii) Thus, in computing the normalized output for the ith node as the ratio of the ith rule's firing strength to the sum of all rules' firing strengths, this process can be expressed as follows:

$$O3,i = \overline{w}i = \frac{wi}{w1 + w2}. \tag{5}$$

2.4. Layer 4: Defuzzy Layer

(i) The nodes in this layer are adaptive in nature.

(ii) For computing the defuzzified output of this layer, the following formula is used:

$$O4,i = \overline{w}ifi = \overline{w}i\,(\alpha ixi + \beta iyi + \gamma i)\,, \tag{6}$$

where αi, βi, and γi refer to the linear or consequent parameters of the corresponding node i.

2.5. Layer 5: Total Output Layer

(i) The single node in this layer provides a synthesis of the information transmitted by layer 4, and it also brings back the overall output using the following fixed function:

$$O5,i = \sum_{i}^{2} \overline{w}ifi, \tag{7}$$

where $i = 1, 2$.

The ANFIS employs a two-pass learning algorithm, namely, forward pass and backward pass. In the first type of pass learning algorithm, no modification of the premise parameters is conducted or carried out; what has to be done is computing the consequent parameters using the least squares estimate learning algorithm. In a similar way, in the backward pass, there is no modification of the consequent parameters, but the process of computing such premise parameters is done by using the gradient descent algorithm. Based on these two learning algorithms, ANFIS adapts the parameters in the adaptive network. From the architecture, it is evident that the overall output of the ANFIS can be represented as a linear combination of the consequent parameters as

$$f = \frac{w1}{w1 + w2} f1 + \frac{w2}{w1 + w2} f2 = \overline{w}1 f1 + \overline{w}2 f2. \tag{8}$$

In the forward pass, the movement of the signals follows forward direction till layer 4 and the consequent parameters are computed, while, in the backward pass, the error rates are propagated backward and the premise parameters are updated by the gradient descent method.

Table 1: Cutting conditions and their levels.

Level	Level code	Cutting speed (m/min)	Feed rate (mm/tooth)	Depth of cut (mm)
Low	−1	50	0.1	1.0
Medium	0	77.5	0.15	1.5
High	+1	105	0.2	2.0

3. Experimental Work

As previously stated, in order to be able to perform its task, an adaptive neuro-fuzzy inference system (ANFIS) needs input-output training patterns. The current study used or adopted the experimental work conducted by Elmagrabi [1] to examine the capability of an adaptive neuro-fuzzy inference system (ANFIS) in predicting surface roughness when end milling *Ti6Al4V* alloy with PVD and uncoated carbide cutting tools under dry cutting conditions. Elmagrabi's study [1] was about developing mathematical models of tool life, resultant cutting forces, and surface roughness in the present study, through integrating Box-Behnken design of experiments with response surface methodology (RSM). This is based on the assumption that a comprehensive overview can contain all the factors which affect the output response by using RSM. Furthermore, this method makes use of a minimum number of experiments, thus is characterized as a money- and time-saving method. Such sets of experiments could cover the problem investigated in the present study.

Table 1 shows the cutting conditions including the cutting speed (m/min), feed rate (mm/min), and depth of cut (mm). Each cutting condition was coded with low, medium, and high levels to cover the problem domains and investigate its effect on surface roughness. The radial depth of cut was maintained constant at 8 mm.

The adoption of a Box-Behnken design in the present study was conducted based on [1]. By doing so, Elmagrabi [1] combined a factorial design of experiments with RSM because of these reasons: the first reason is that such kind of experimental design does not need or require many points of design and it is regarded as a design which costs less than central composite design by using almost the same number of factors; the second reason is that this type of design does not have axial points, and, therefore, there would not be simultaneous setting of all cutting parameters levels

Table 2: Experimental results used in training phase.

No.	Cutting speed (m/min)	Feed rate (mm/rev)	Depth of cut (mm)	Surface roughness (μm)	
				PVD	Uncoated
1	77.5	0.1	1	0.55	0.55
2	105	0.1	1.5	0.35	0.666
3	77.5	0.15	1.5	0.9	0.783
4	77.5	0.15	1.5	0.86	0.85
5	50	0.15	1	0.72	0.565
6	77.5	0.2	1	1.32	1.426
7	105	0.15	2	0.8	0.767
8	105	0.2	1.5	1.32	1.912
9	50	0.15	2	0.7	1.173
10	105	0.15	1	0.58	0.84
11	77.5	0.15	1.5	0.9	0.673
12	50	0.2	1.5	0.8	1.444
13	77.5	0.2	2	0.91	1.66
14	77.5	0.1	2	1.32	0.856

Table 3: Experimental data used in testing phase.

No.	Cutting speed (m/min)	Feed rate (mm/rev)	Depth of cut (mm)	Surface roughness (μm)	
				PVD	Uncoated
1	50	0.1	1.5	1.212	0.872
2	77.5	0.15	1.5	0.81	0.796
3	77.5	0.15	1.5	1	0.900

Figure 4: CNC Milling Machine.

at higher levels and all the design points would be located in the safe operating zone. Moreover, in using this design, only five design points were replicated so that the effects and interactions among the three independent cutting parameters could be investigated. Putting what was mentioned above into application, 17 data sets were created based on this design of the experiments. The experimental data were divided into two sets: one set for training (Table 2) and the other for testing or checking (Table 3). As displayed in Figure 4, Cincinnati Milacron Vertical CNC Milling Machine (model Sabre 750 with Acramatic 850 SX) was used for the purpose of machining *Ti6Al4V* alloy. In carrying out the milling process, it was conducted under dry cutting conditions by using PVD (Ti-Al-N) coated and uncoated carbide cutting tools. The mechanical features of *Ti6Al4V* alloy and tool geometry are provided in Tables 4 and 5, respectively. The current study adopted the arithmetic surface roughness (R_a), and its measurement was conducted on the machined surface which was parallel to the feed motion with a portable surface roughness tester (Mpi Maher perthometer model) as displayed in Figure 5.

Measuring the arithmetic surface roughness (R_a), was carried out online with a portable surface tester, and its measurement was taken after each pass. To obtain the R_a values of the machined surface, the surface roughness values have been averaged at three locations on the centre path of the work piece width. In order to calibrate the instrument, the setting of the roughness width cutoff based on the roughness value expected was needed or required. Selection of the width cutoff was done as 0.8 mm, and the failure criterion for the tool was maintained at 6 μm surface roughness.

4. Result and Discussion

Like any AI techniques, the ANFIS model requires two different sets of data: training data sets and testing data sets. The present study made use of or utilized the experimental data shown in Table 2 in the training phase, whereas the experimental data of Table 3 was used in the testing phase. Figure 6 displays the flow chart of training of ANFIS. The study

Table 4: Mechanical properties of *Ti6Al4V* alloy.

Ultimate tensile strength MPa	Yield strength MPa	Rockwell hardness HRC	Modulus of elasticity GPa	Poisson's ratio
950	880	36	113.8	0.342

Table 5: PVD coated and uncoated carbide specifications.

ISO grade K20	Insert cutting rake angle	Insert side clearance angle	Insert helix angle	Insert radius
(S20–S30)-XOMX090308TR ME06, F40 (PVD coated carbide Ti-Al-N) with chamfer of 0.06 width at 4°	24°	11°	15°	8 mm
(S20)-XOMX090308TR ME06, H25 (uncoated carbide) with chamfer of 0.06 width at 4°	24°	11°	15°	8 mm

Figure 5: Surface roughness tester.

used the architecture of ANFIS which adopted a generalized bell-shaped function as shown in Figure 7. As it is noticed, this architecture consisted of 8 fuzzy rules.

In carrying out the training process, the researcher chose the generalized bell-shaped (gbell) function as a membership function being numbered as 2, 3, 4, and 5 to show its impacts on the prediction accuracy. Epochs were changed from 50 up to 1000. 160 ANFIS models were developed for two cases, that is, coated and uncoated cutting tools, and selection of the best models was carried out based on the minimum root mean square error in the testing phase. After the training and testing phases were accomplished, only six models was chosen and each three models were chosen for evaluating the model for each case. Tables 6 and 7 present the ANFIS parameters for each model.

Based on recommendation or suggestions by previous review, the step-size profile was made in a form or shape of a curve in that it increased at first, then, reached some maximum point, and finally decreased for the rest of the training. It was gained through tuning the initial step size and the increase and decrease of rates.

As shown in Tables 8 and 9, the predicted results obtained from the experiments of the three ANFIS models for both

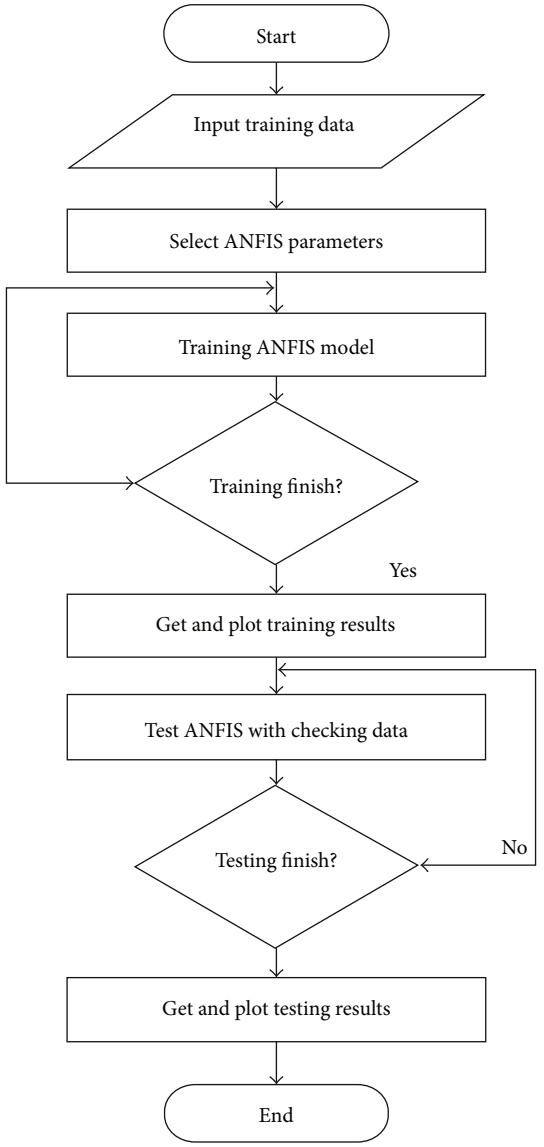

Figure 6: Flowchart of ANFIS training.

Table 6: ANFIS parameters for PVD coated carbide.

ANFIS models	Type of membership function	No. of membership functions	Epochs	Number of nodes	Number of linear parameters	Number of nonlinear parameters	Total number of parameters	Number of fuzzy rules	Step size
A	gbell	2	50	34	32	18	50	8	0.01
B	gbell	2	100	34	32	18	50	8	0.01
C	gbell	2	150	34	32	18	50	8	0.01

Table 7: ANFIS parameters for uncoated carbide.

ANFIS models	Type of membership function	No. of membership functions	Epochs	Number of nodes	Number of linear parameters	Number of nonlinear parameters	Total number of parameters	Number of fuzzy rules	Step size
A	gbell	2	100	34	32	18	50	8	0.01
B	gbell	2	150	34	32	18	50	8	0.01
C	gbell	2	250	34	32	18	50	8	0.01

Table 8: Experimental and ANFIS results of PVD coated cutting tool.

No.	Cutting speed (m/min)	Feed rate (mm/tooth)	Depth of cut (mm)	Surface roughness (μm)	Model A	Model B	Model C
1	77.5	0.1	1	0.55	0.55	0.55	0.55
2	105	0.1	1.5	0.35	0.350001	0.350001	0.350001
3	77.5	0.15	1.5	0.9	0.886667	0.886667	0.886667
4	77.5	0.15	1.5	0.86	0.886667	0.886667	0.886667
5	50	0.15	1	0.72	0.719999	0.719999	0.719999
6	77.5	0.2	1	1.32	1.32	1.32	1.32
7	105	0.15	2	0.8	0.8	0.8	0.8
8	105	0.2	1.5	1.32	1.32	1.32	1.32
9	50	0.15	2	0.7	0.700001	0.700001	0.700001
10	105	0.15	1	0.58	0.579999	0.579999	0.579999
11	77.5	0.15	1.5	0.9	0.886667	0.886667	0.886667
12	50	0.2	1.5	0.8	0.8	0.8	0.8
13	77.5	0.2	2	0.91	0.91	0.91	0.91
14	77.5	0.1	2	1.32	1.319998	1.319998	1.319998

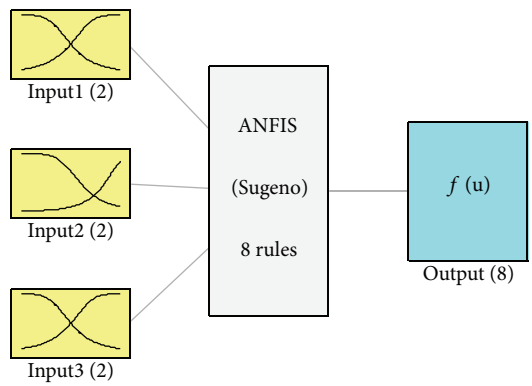

Figure 7: ANFIS architecture with gbell membership function.

Table 9: Experimental and ANFIS results of uncoated cutting tool.

No.	Cutting speed (m/min)	Feed rate (mm/tooth)	Depth of cut (mm)	Surface roughness (μm)	Model A	Model B	Model C
1	77.5	0.1	1	0.55	0.55	0.55	0.55
2	105	0.1	1.5	0.666	0.666	0.666	0.666
3	77.5	0.15	1.5	0.783	0.768667	0.768667	0.768667
4	77.5	0.15	1.5	0.85	0.768667	0.768667	0.768667
5	50	0.15	1	0.565	0.565	0.564999	0.565
6	77.5	0.2	1	1.426	1.426001	1.426	1.426
7	105	0.15	2	0.767	0.767	0.767	0.767
8	105	0.2	1.5	1.912	1.912	1.911999	1.912
9	50	0.15	2	1.173	1.172999	1.173	1.173
10	105	0.15	1	0.84	0.84	0.84	0.84
11	77.5	0.15	1.5	0.673	0.768667	0.768667	0.768667
12	50	0.2	1.5	1.444	1.443999	1.443999	1.443999
13	77.5	0.2	2	1.66	1.660001	1.660001	1.660001
14	77.5	0.1	2	0.856	0.856	0.856	0.856

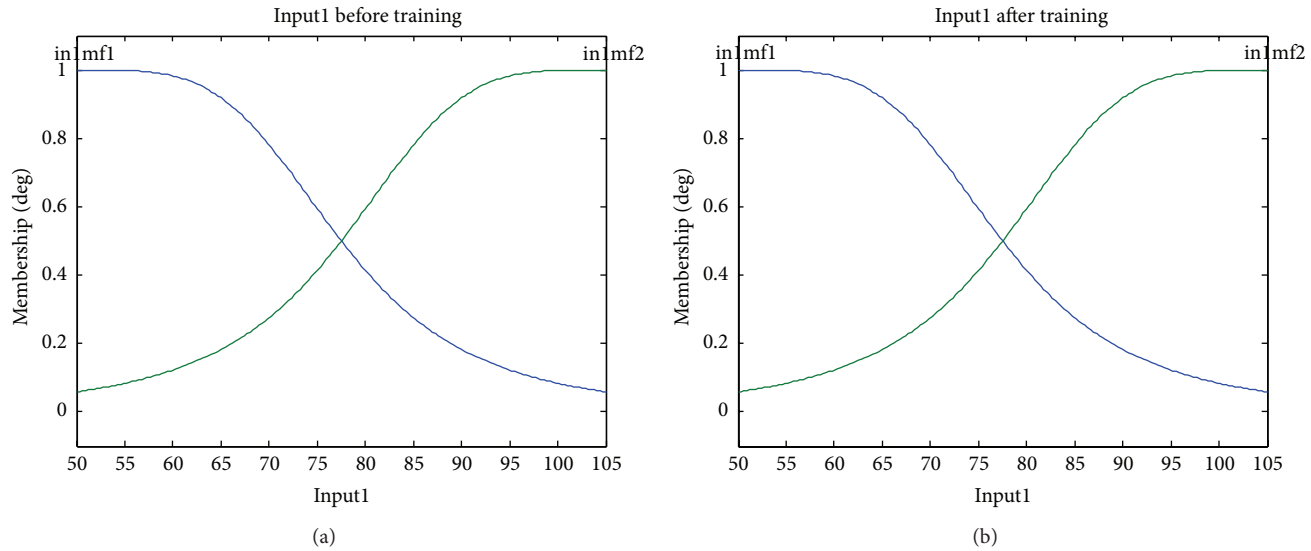

(a) (b)

Figure 8: Membership functions of cutting speed before and after training (Model A, PVD).

PVD coated and uncoated cutting tools are presented. Findings revealed that, in general, the experimental and predicted results for all six models in the training phase matched each other well.

The minimum root mean square error (RMSE) was used as a criterion for selecting the best two models for coated and uncoated tools among the six ones, and the results concerning the different values of the RMSE for the six models are presented in Table 10.

According to the above results, the minimum RMSE for PVD cutting tool is 0.2412 (Model A) while the minimum RMSE for uncoated tool is 0.1030 (Model A). Therefore, based on these values, the two models were selected as the best ANFIS models in prediction surface roughness using coated and uncoated cutting tools.

Table 10: RMSE of the selected models.

ANFIS Models	RMSE/PVD	RMSE/Uncoated
A	**0.2412**	**0.1030**
B	0.2477	0.1067
C	0.2477	0.1056

Figures 8, 9, and 10 display the results concerning the membership functions of the model A in the pretraining and posttraining stages for three input parameters, namely,

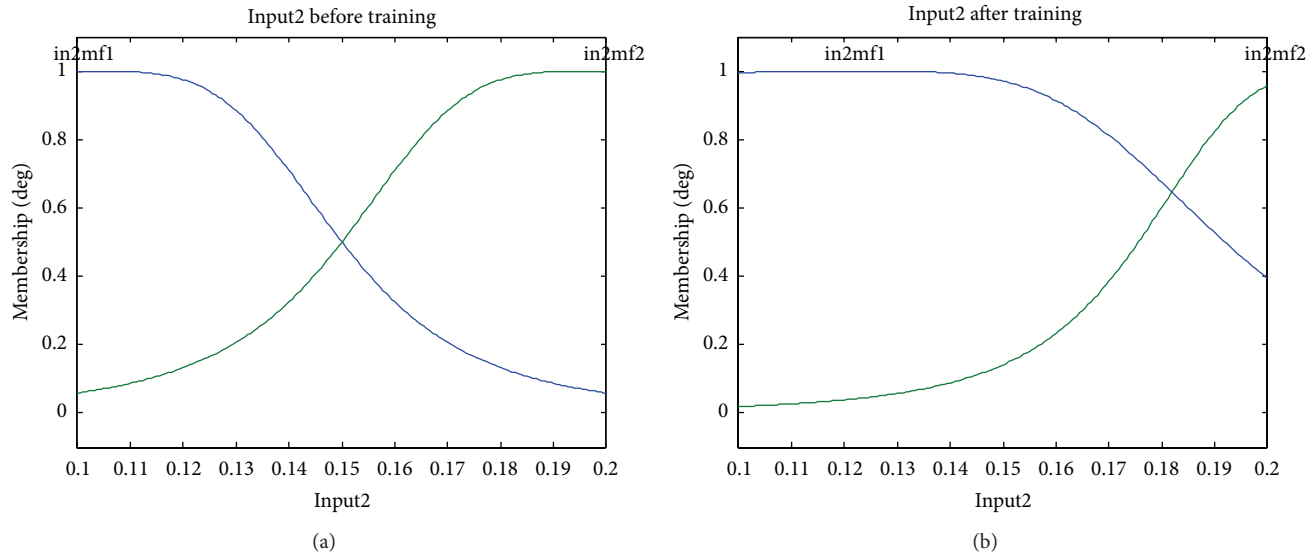

Figure 9: Membership functions of feed rate before and after training (Model A, PVD).

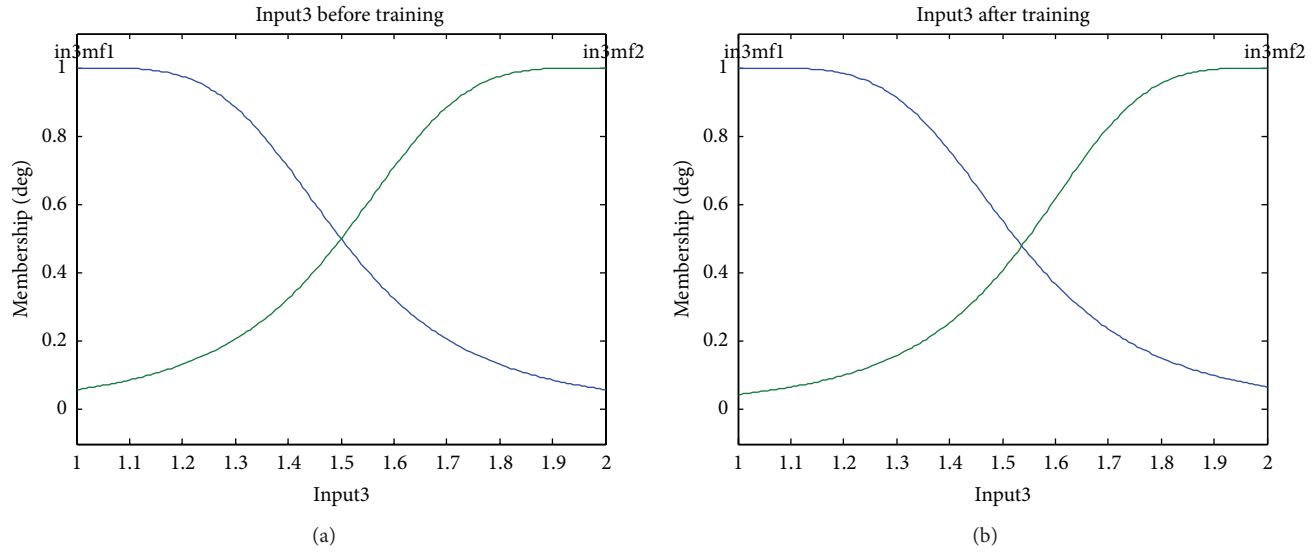

Figure 10: Membership functions of depth of cut before and after training (Model A, PVD).

cutting speed, feed rate, and depth of cut, respectively. The findings provided evidence of a huge change occurred to the membership functions of feed rates, but the change in those of the depth of cut was slight. Such results imply that the feed rate is the factor which most significantly affects the surface roughness when using coated tool followed by depth of cut.

Figures 11, 12, and 13 displayed the results concerning the effect of those factors on the surface roughness, and as shown in Figures 9–11, the highest effect on the surface roughness was exerted by the feed rate when using uncoated carbide cutting tool to machine *Ti6Al4V* alloy. Closely looking at the results presented in Table 2 and the ANFIS results, it can be summed up that the most significant effects on the surface roughness were exerted by feed rate followed by depth of cut. In obtaining good surface finish, both the feed rate and depth of cut should be at level (−1) and cutting speed at level (+1), respectively. Such important findings are consistent with the findings obtained by Elmagrabi [1]. It is clear from Tables 2 and 3 that the surface roughness values of the milled Ti6Al4V alloy are different for the two cutting tools. The reasons beyond that difference return to the fact that the insert type has significant effect on surface roughness in addition to cutting conditions and other parameters. Moreover, the Ti-Al-N coated layer which acts as dry lubricant for the PVD coated insert resulted in good surface finish especially at low feed rate and high cutting speed. On the other hand, the high surface roughness values for uncoated insert, are probably due to pronounced chipping, flaking of the sharp edge.

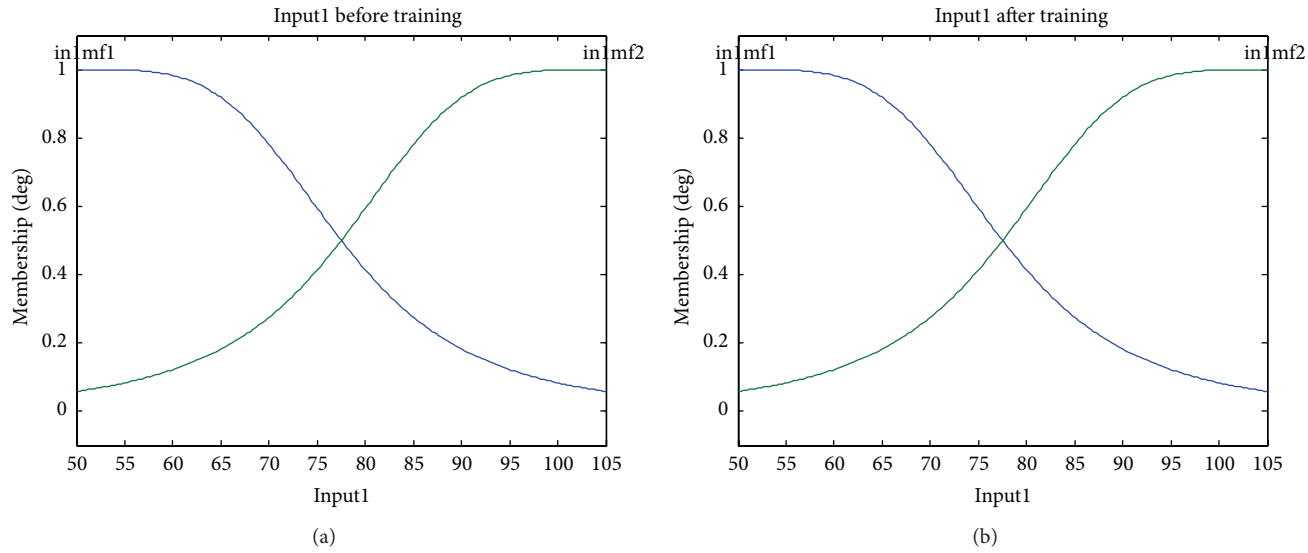

Figure 11: Membership functions of cutting speed before and after training (Model A, uncoated).

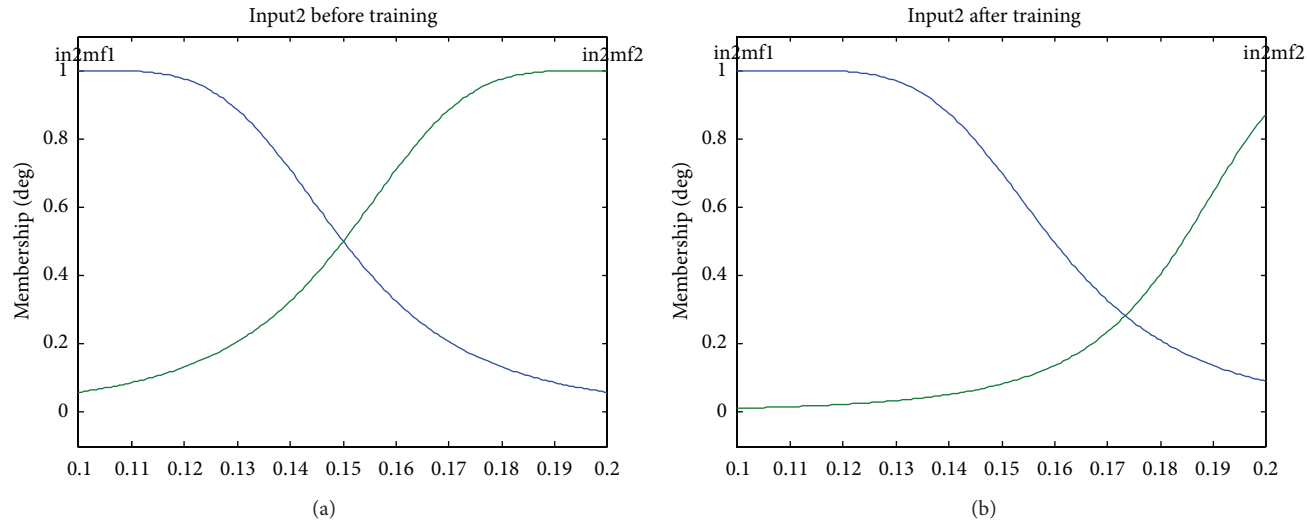

Figure 12: Membership functions of feed rate before and after training (Model A, uncoated).

Figures 14 and 15 display the results obtained through the best two models in the training phase, respectively. The most effective and best matching training phase and minimum RMSE in testing phase were given by the two models. Figures 16 and 17 show the scatter diagram for the measured and predicted results in training phase for coated and uncoated cutting tools. Based on these findings, a good agreement between the experimental and predicated values was evidently proven and the data followed 45° line.

5. Conclusion

The present study examined the application of the ANFIS in prediction of the surface roughness when end milling *Ti6Al4V* alloy with coated and uncoated cutting tool under dry cutting conditions. Among many ANFIS models that have been developed and tested in the current experimental work, only two models were chosen as the best models in making prediction of the surface roughness generated through the cutting process. The findings showed that Model A with gbell membership function and 50 epochs obtained a minimum RMSE of 0.2412 for the PVD coated tool. However, the same model with the same membership function and 100 epochs obtained a minimum RMSE of 0.1030. Although the data sets used for training and testing in the present study were lower than those used in other previous studies, the study obtained good results, thus providing evidence of

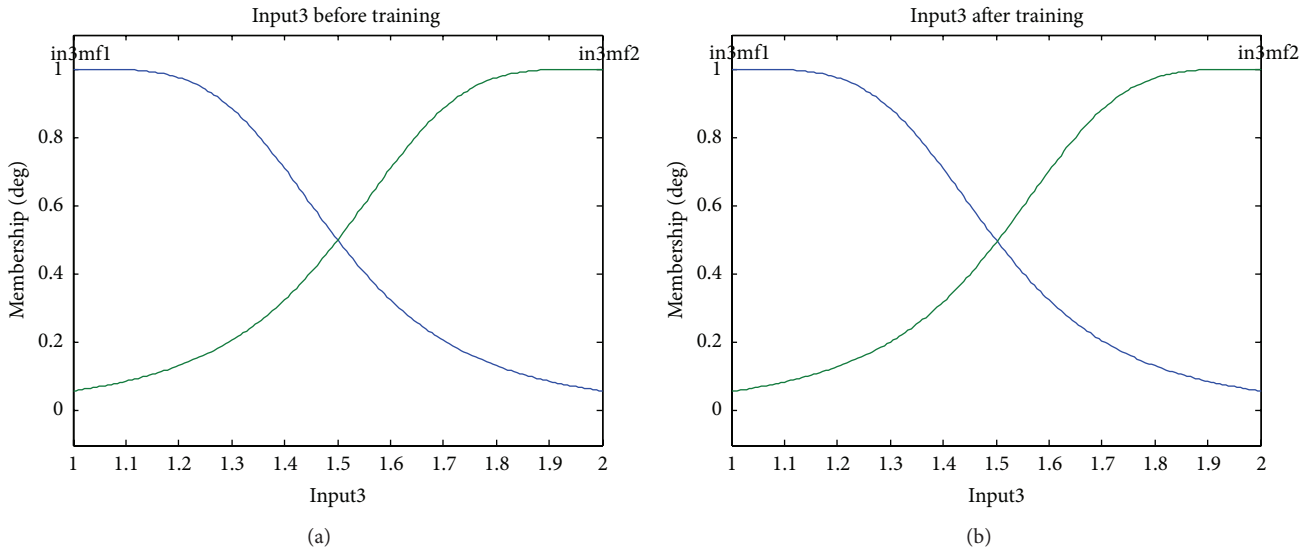

Figure 13: Membership functions of depth of cut before and after training (Model A, uncoated).

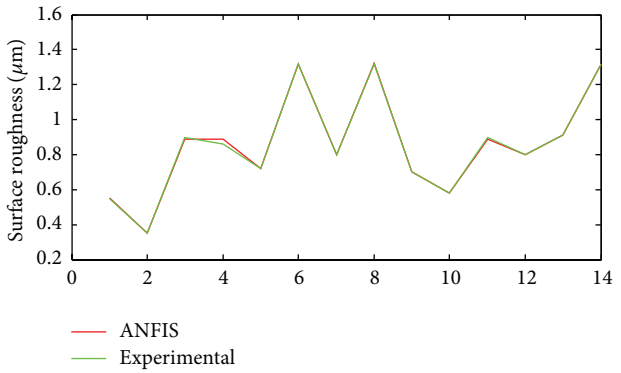

Figure 14: Experimental and predicted results of Model A, PVD.

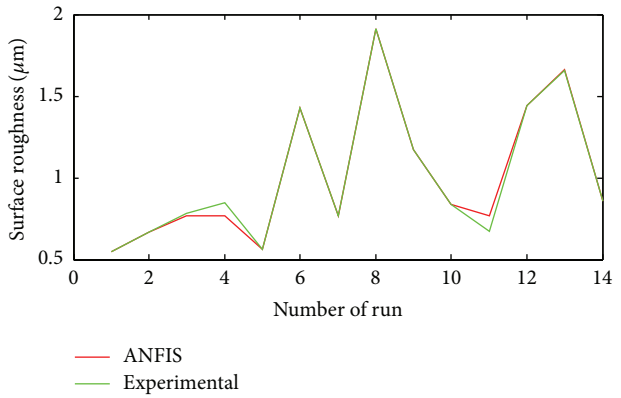

Figure 15: Experimental and predicted results of Model A, uncoated.

the efficient use of such models in predicting the surface roughness.

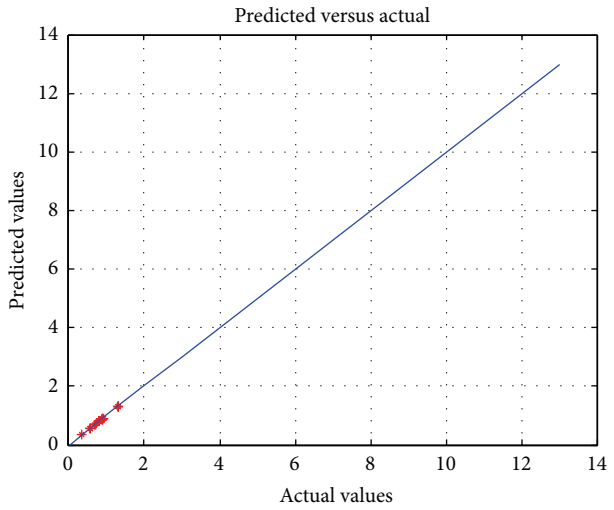

Figure 16: Actual and predicted values for PVD coated carbide.

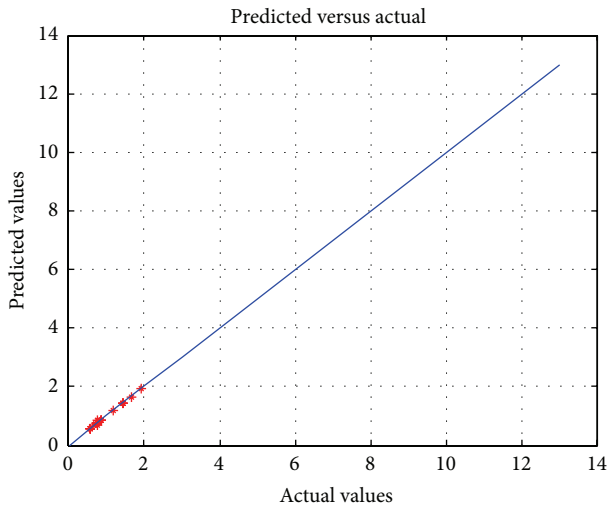

Figure 17: Actual and predicted values for uncoated cutting tool.

Abbreviations

ANFIS:	Adaptive neurofuzzy inference system
GP:	Genetic programming
ANN:	Artificial neural network
RSM:	Response surface methodology
RMSE:	Root mean square error
x, y:	Inputs of the ANFIS
f:	Output of the ANFIS
$\alpha 1$, $\beta 1$, $\gamma 1$, $\alpha 2$, $\beta 2$, and $\gamma 2$:	Linear parameters
$A1$, $B1$, $A2$, and $B2$:	Non linear parameters
$O1, i$:	Output of the ith node
$O2$, j:	Output of the jth node
μAi, μBi:	Membership function of the inputs
$O3, i = \overline{w}i$:	Normalised weight function of normalised layer
$O4, i$:	Output of defuzzy layer
$O5, i$:	Output of the output layer.

References

[1] N. H. E. Elmagrabi, *End Milling of Titanium Alloy Ti-6Al-4V With Carbide Tools Using Response Surface Methodology*, Universiti Kebangsaan, Bangi, Malaysia, 2009.

[2] J. Sun and Y. B. Guo, "A comprehensive experimental study on surface integrity by end milling *Ti-6Al-4V*," *Journal of Materials Processing Technology*, vol. 209, no. 8, pp. 4036–4042, 2009.

[3] P. G. Benardos and G. C. Vosniakos, "Prediction of surface roughness in CNC face milling using neural networks and Taguchi's design of experiments," *Robotics and Computer-Integrated Manufacturing*, vol. 18, no. 5-6, pp. 343–354, 2002.

[4] A. M. Zain, H. Haron, and S. Sharif, "Prediction of surface roughness in the end milling machining using artificial neural network," *Expert Systems with Applications*, vol. 37, no. 2, pp. 1755–1768, 2010.

[5] T. Erzurumlu and H. Oktem, "Comparison of response surface model with neural network in determining the surface quality of moulded parts," *Materials and Design*, vol. 28, no. 2, pp. 459–465, 2007.

[6] P. Benardos, "Predicting surface roughness in machining: a review," *International Journal of Machine Tools and Manufacture*, vol. 43, no. 8, pp. 833–844, 2003.

[7] V. Dhokia, S. Kumar, P. Vichare, and S. Newman, "An intelligent approach for the prediction of surface roughness in ball-end machining of polypropylene," *Robotics and Computer-Integrated Manufacturing*, vol. 24, no. 6, pp. 835–842, 2008.

[8] A. K. M. N. Amin, A. F. Ismail, and M. K. Nor Khairusshima, "Effectiveness of uncoated WC-Co and PCD inserts in end milling of titanium alloy-*Ti-6Al-4V*," *Journal of Materials Processing Technology*, vol. 192-193, pp. 147–158, 2007.

[9] S. sumathi and S. Paneerselvam, *Computational Intelligence Paradigms Theory and Applications Using MATLAB*, Taylor & Francis, Boca Raton, Fla, USA, 2010.

[10] J. S. R. Jang, "*ANFIS*: adaptive-network-based fuzzy inference system," *IEEE Transactions on Systems, Man and Cybernetics*, vol. 23, no. 3, pp. 665–685, 1993.

[11] S. N. Sivanandam and S. Deepa, *Introduction to Neural Networks Using MATLAB 6. 0*, Tata McGraw-Hill, Delhi, India, 2006.

[12] U. Zuperl, F. Cus, B. Mursec, and T. Ploj, "A generalized neural network model of ball-end milling force system," *Journal of Materials Processing Technology*, vol. 175, no. 1–3, pp. 98–108, 2006.

[13] F. Dweiri, M. Al-Jarrah, and H. Al-Wedyan, "Fuzzy surface roughness modeling of CNC down milling of Alumic-79," *Journal of Materials Processing Technology*, vol. 133, no. 3, pp. 266–275, 2003.

[14] S. Lo, "An adaptive-network based fuzzy inference system for prediction of workpiece surface roughness in end milling," *Journal of Materials Processing Technology*, vol. 142, no. 3, pp. 665–675, 2003.

[15] C. Göloğlu and Y. Arslan, "Zigzag machining surface roughness modelling using evolutionary approach," *Journal of Intelligent Manufacturing*, vol. 20, no. 2, pp. 203–210, 2008.

[16] W.-H. Ho, J.-T. Tsai, B.-T. Lin, and J.-H. Chou, "Adaptive network-based fuzzy inference system for prediction of surface roughness in end milling process using hybrid Taguchi-genetic learning algorithm," *Expert Systems with Applications*, vol. 36, no. 2, pp. 3216–3222, 2009.

[17] Z. Uros, C. Franc, and K. Edi, "Adaptive network based inference system for estimation of flank wear in end-milling," *Journal of Materials Processing Technology*, vol. 209, no. 3, pp. 1504–1511, 2009.

[18] M. Dong and N. Wang, "Adaptive network-based fuzzy inference system with leave-one-out cross-validation approach for prediction of surface roughness," *Applied Mathematical Modelling*, vol. 35, no. 3, pp. 1024–1035, 2011.